

Application of the PS-InSAR Technique for the Post-Failure Landslide Deformation Monitoring at Lubietova Site in Central Slovakia

Vladimir Greif and Jan Vlcko

Abstract

The interferometric synthetic aperture radar data from ERS and ENVISAT sensors were utilized in the analysis of the post-failure deformations in the area of Lubietova town in Central Slovakia. The catastrophic landslide of 1977 together with surrounding landslides in the Lubietova area were analysed with the help of persistent scatterers (PS) technique in order to evaluate recent and past deformations of the unstable slopes. Although long-term precise geodetic monitoring of the 1977 landslide revealed differential deformations inside the sliding mass, due to the lack of the PS located inside the landslide caused by temporal decorrelation, unfortunately these records could not be directly compared. The adjacent landslides with sufficient number of PS were analysed by transformation of the line of sight displacements recorded by the sensors to the slope vector direction. This procedure allowed identification of the precise boundaries of the actively moving landslide parts and the updating of the landslide inventory for the Lubietova area.

Keywords

Landslide monitoring • PS-InSAR • Radar interferometry • Lubietova

Introduction

Slow-moving landslides pose a challenge for the engineer, due to the difficulty of distinguishing their mechanism and simultaneously the inability to determine the exact area which will be affected by these phenomena. Prediction of displacement rate increase is very problematic and thus the assessment of future behaviour is almost impossible.

Remote satellite techniques have been routinely used for landslide mapping and monitoring for some time, and optical imagery and GPS techniques are well established methods in studying the geomorphology and topography of landslides including monitoring slope deformation (Malet et al. 2002).

In comparison, the idea of the exploitation of satellite-born radar sensors is quite new. The practical use of radar techniques in landslide study originated in 1989 when differential interferometric synthetic aperture radar technique (DInSAR) was described by Gabriel et al. (1989). Early attempts used few interferograms which provided flexibility in assessing the ground deformations even in conditions of limited SAR data availability. The original DInSAR consisted of only two SAR data acquisitions and it contained at least two inherent errors in interferogram creation. Firstly atmospheric variations affected radar wave phase delay and secondly, the digital elevation model used for cancellation of the topography created from two-pass signal interference was inaccurate. Following analysis of a multitemporal and multibaseline stack of interferograms, Ferretti et al. (1999, 2001) came up with the idea of using longer acquisition sequences to overcome this limitation. This technique was called Permanent Scatterers (PS) and it mitigated the Atmospheric Phase Delay (APD) via statistical filtering of long-term radar sequences. It also provided residual

V. Greif (✉) • J. Vlcko

Department of Engineering Geology, Faculty of Natural Sciences,
Comenius University in Bratislava, Mlynska Dolina G, Bratislava,
Slovakia

e-mail: greif@fns.uniba.sk

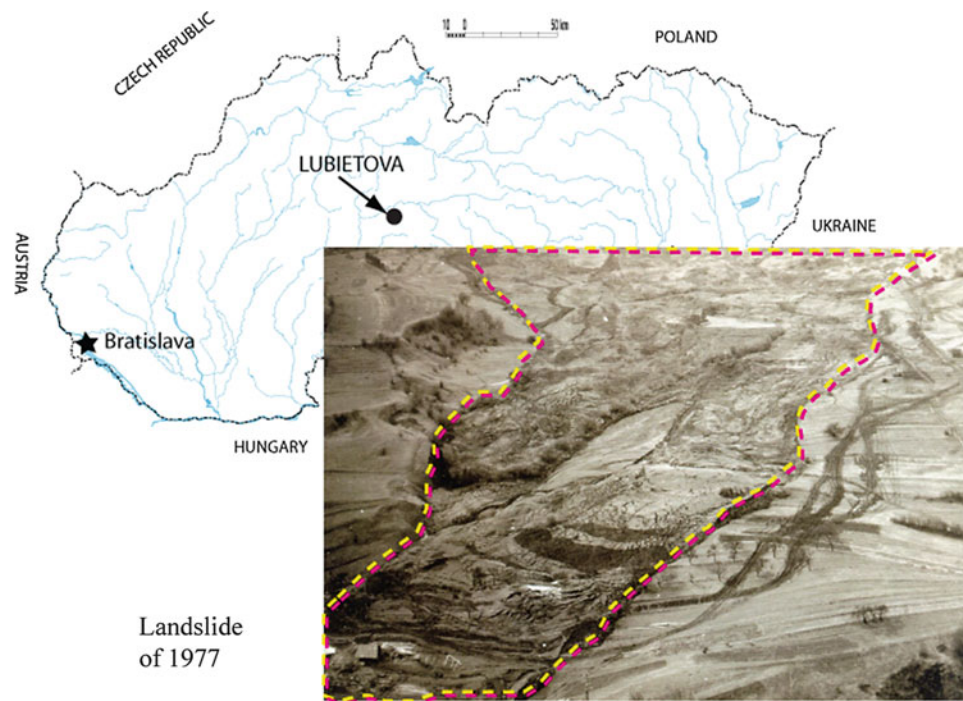


Fig. 1 Localization of the study site with the photo of the catastrophic Lubietova landslide taken shortly after the event

topography estimates with very high accuracy on stable targets. More recently intensive research and development in the field of algorithms and procedures for PS analysis was introduced (Berardino et al. 2002; Mora et al. 2003; Wegmüller et al. 2005; Kampes and Adam 2005; Fornaro et al. 2007; Guarnieri and Tebaldini 2008).

The DInSAR technique has detailed description in scientific literature (Rott and Nagler 2006; Colesanti and Wasowski 2006), and it has been successfully used in subsidence study (Ferretti et al. 2000; Henry et al. 2004; Amelung et al. 1999; Rott et al. 2002,2003), co-earthquake deformation analysis, volcano monitoring and for other purposes.

The first application of DInSAR in landslide study was reported from France (Fruneau et al. 1996), followed by Canada (Singhroy et al. 1998), Austria (Rott et al. 1999) and other areas (Vietmeier et al. 1999; Crosetto et al. 2005). The improved PS-InSAR is especially useful in landslide monitoring where the deformation rates are less than approx. 1.4 cm/month and long term series of SAR data is available (Colesanti et al. 2003; Colesanti and Wasowski 2004; Hilley et al. 2004; Bovenga et al. 2006; Farina et al. 2006, 2008; Herrera et al. 2009). PS-InSAR is capable of detecting deformations of individual objects from “small” individual houses to objects only about 1 m² in size. A certain density of stable objects (about 5 per km²) is needed to enable accurate correction of APD (Singhroy 2009). One significant advantage beside the price per sq. km, is the existence of an archive of SAR data allowing monitoring of favourably oriented landslides or other phenomena as far back as July 1991

(Hasager et al. 2002). However, the following challenges remain to be solved, according to Colesanti and Wasowski 2006; Rocca 2003; Manzo et al. 2006:

1. PS data represent a one-dimensional line of sight (1D LOS) projection of a deformation occurring in a 3D world. Some attempts to resolve horizontal displacements from 1D LOS were carried out by Cascini et al. (2010);
2. Deformation greater than $\lambda/4$ between two following visits of the satellite are difficult to track due to the ambiguity of radar phase measurements;
3. The measurements are limited due to the positioning of PS and the re-appearance time intervals of the satellite;
4. While it is possible to obtain high density PS in urban areas, it is very difficult to obtain coherent density of pixels in rural areas where most landslides occur. This was addressed by the use of artificial corner reflectors (Ye et al. 2004; Novali et al. 2005), which had the accompanying shortcoming of loss of availability of archive SAR data.

Herein, the authors adopt the PS-InSAR technique in the study of post-failure behaviour in the landslide area near Lubietova in Central Slovakia.

Geological Settings

Lubietova village is located in Central Slovakia about 16 km east of the third largest Slovak city Banská Bystrica (Fig. 1).

During the middle ages, the town of Lubietova was one of the seven most important mining towns in the Upper Hungarian monarchy. The town was famous for its rich abundance of copper ore mined there in fourteenth and fifteenth Centuries, with the mineral Libethenite being a rare secondary copper phosphate hydroxide which derived its name from the formal German name of this town – Libethen.

The studied site is situated in the narrow valley of the Hutna River between the two ranges of the Slovenske Stredohorie Mountains on the west and the Slovenske Rudohorie Mountains on the east. The hillsides dip at gentle slopes at altitudes from 450 to 700 m a.s.l. The eastern aspect slopes are composed of Lower Triassic quartzites, conglomerates and sandstones, and also dolomitic breccias and dolomites. The upper horizons consist of Quaternary clays and slope detritic loams. The bedrock of the opposite slopes of the valley is formed by the Inner-Carpatian Paleogene flysch strata consisting mainly of highly weathered claystones with occasional interbeds of sandy layers. Andesitic epiclastic breccias and conglomerates of Neogene age outcrop at the higher altitudes of the western facing slopes and these form the geomorphologically active parts of the mountain ridge. They rest on a Paleogene clay strata which forms favourable conditions for slow slope deformations. From the geodynamic point of view, these slopes are prone to sliding and this is in stark comparison to the eastern slopes of quartzite and dolomite rocks where stable conditions prevail.

Catastrophic Landslide of Lubietova in 1977

Lubietova landslide (L1) (Fig. 1) occurred in the spring of 1977 (February–April), following a precipitation anomaly lasting from December 1976 to the end of February 1977, when the average monthly precipitation recorded 150–220 % of the long-term average. This precipitation combined with melting snow and triggered an earth flow of asymmetric shape covering an area of approximately 30 ha. The detachment area consisted of three separate detachment zones which merged into an earth flow with the deposition zone partly damming the Hutna River. The altitude difference between the detachment and accumulation zones was 170 m while the length of the earth flow was 1,230 m. The largest width of 400 m in the detachment zone narrowed to 100 m where the river obstruction occurred. Velocities measured during the first days after the occurrence of the landslide reached 2.5 m/day and total recorded displacements were about 9 m, 42.9 m, and 3–6 m in the detachment, transportation and accumulation zones respectively. The sliding surface depths varied dependent on the location from 30 m near the landslide scarp, 15–20 m in the transportation area and 6–8 m in the deposition zone.

The total displaced mass measured about 4.5 million cubic metres of deluvial clays (Nemčok 1982). The recent study carried out by Prokesova et al. (2010) using sequential sets of high resolution aerial photographs of this area estimated the displaced mass balance between 1969–1977 and $-111,400/+91,500 \text{ m}^3$. In order to minimize the risk of the river damming during the landslide's maximal activity, several large diameter steel pipes were placed in the river bed allowing the river to flow unobstructed by sliding masses.

The bedrock geology in the vicinity of the landslide is rather complex, with Lower Triassic massive quartzite rocks found in the accumulation zone and Paleogene Flysch-like sediments overlain by slope sediments in the transportation and detachment zones. The Paleogene claystones and shales dip $5\text{--}15^\circ$ towards the northeast creating predisposing shear planes. In the close vicinity of the catastrophic landslide there were several displaced huge blocks of Neogene vulcanoclastics in the form of lateral spreads giving the potential for extremely slow slides.

Shortly after this catastrophic event stabilization works were recommended and applied. Surface drainage and sub-horizontal drainage boreholes to decrease the water level inside the sliding body together with buttress-fill grading were installed at the accumulation zone in order to stabilise the area. Following this event a deeper study was carried out by Malgot (1978), who identified several landslides on the western slopes and classified them according to their type and activity. This catastrophic landslide has been continuously monitored since 1988 by precise geodetic measurements and by recording the water level inside the boreholes located within the landslide boundaries.

In a more recent study, Vlcko et al. (2001) adopted a different approach in landslide hazard assessment of the studied area. In the first stage, a traditional landslide distribution map was compiled and this served for further landslide risk map elaboration based on quantitative analysis using the geotechnical approach. This geotechnical, or deterministic, approach was based on the calculation of the safety factor of each landslide body in relation to the designed type of buildings on the urban plan. Since the majority of residential houses were located in the accumulation part of the currently dormant landslides, the calculation was based on foundation dimensions of $12 \times 12 \times 3 \text{ m}$. The final landslide risk zones in the map were delineated according to the factor of safety (FOS) calculated for each landslide separately. The FOS for the L1 landslide using the soil parameters from a previous survey carried out by Jadroň et al. 1975 was 1.023 when stabilization measures were not taken into account. This illustrates the susceptibility to sliding of the western-facing slopes of the valley formed of clays, clayey loams and shales, which were overlain by Neovolcanic rock caps in some areas. Subsequent

deformations inside the landslide body had a negative effect on the stabilization measures. This particularly applied to the surface drainage channels which were displaced, thus losing functionality. The effectiveness of the subsurface drainage boreholes was limited due to this same reason and re-activation of the landslide is merely a matter of time according to Míka (1999).

Post-Failure Geodetic Monitoring

In 1988, the Geological Survey of Slovakia installed a geodetic monitoring network of more than 30 geodetic points (GP) located inside the L1 landslide body to track the post-failure development of the failure to discover if the sliding body posed a threat to the inhabitants and their property. The geodetic points were monitored by precise geodetic surveys beginning in 1988 and carried out at irregular time intervals. The survey still continues and the results for the period 1988–2006 are shown in Fig. 2. The displacement rates for 30 GP's were calculated from the changes of their coordinates over time by calculating the slopes of the linear regression lines for each X, Y, and Z coordinates separately. Figure 2 shows the projection of the displacement rates in an XY plane.

Higher post-failure velocities were recorded in the northern part of the landslide body reaching values up to the 10 mm/year, while the southern parts are moving at slower rates from 1 to 3 mm/year. This shows a differential distribution of the deformation within one sliding mass. The results of this monitoring campaign were intended to be a benchmark to compare results of the PS-InSAR monitoring, in order to evaluate the displacement rates of PS.

PS Technique Results

Three datasets were used for the PS analysis consisting of 50 scenes (track 451) from ERS 1, 2 acquired between 1993–2000 and 58 scenes (track 415, 451) from the ENVISAT two satellite, acquired between the 2002 and 2009. The ENVISAT scenes were from both ascending and descending acquisition orbits, while the ERS1, 2 images were taken only from the descending orbit. The number of derived PS targets for the 4.5 km² area of interest was 1683 (455 PS – ENVISAT/Asc., 787 PS – ENVISAT/Desc. and 441 PS – ERS/Desc.). The PS processing was performed by Telerilevamento Europa and satellite images were provided under EC/ESA GSC-DA within the FP7 GMES SAFER project. The three data stacks were processed by means of PSInSAR technique using PSI approach developed by Polytechnic University of Milan and licensed to TRE Europa. A simple linear model of phase variation through

time was used for estimation of phase components related to deformations. For the DEM (Digital Elevation Model) correction a SRTM (Shuttle Radar Topography Mission) DEM with 3 arc seconds resolution produced by NASA was used. For each data set a reference point exhibiting no displacement located in the presumably stable area in the fluvial sediments near the town centre was selected. All PS displacements in the data set were referred to this point.

The average density of PS is approx. 374 PS/km², which represents a rather high density considering that the studied site is a rural area. Most of the PS targets were located, as expected, on man-made structures such as steel roofs, houses, and bridges in the town, while the landslides were unfortunately lacking scatter points due to temporal de-correlation. The catastrophic landslide of 1977, located in the northwestern part of the town does not contain any reflection points, while the other two, landslides 2 and 3, have the PS located mainly in the accumulation zone. The distributions of the PS and their LOS displacement rates from both satellites are shown in Fig. 3. The hilly parts of the area had PS located on rocky outcrops, showing very slow movements in the LOS direction and mainly corresponding to deep seated deformations of a creep character.

The 1D LOS displacement rates in the studied area vary in range from –5 to +5 mm/year, with the negative values indicating displacements away from the radar sensor along the line of sight direction. From the PS located in the area of the landslides 2 (L2) and 3 (L3) most of the targets are located in the accumulation zone with gentle slope. These targets have an LOS displacement rate below the 2 mm/year, which some authors such as Colesanti and Wasowski (2006); and Righini et al. 2009 consider to be the threshold between stable and unstable states of sliding. Nevertheless, it is possible to trace the boundary between the slowly creeping areas and the stable parts of the landslide mass.

Discussion and Conclusions

The use of the PS-InSAR technique for the identification of unstable areas proved to be a very cost-efficient method in large areas, where sufficient number of PS can be found (Van der Kooij 1999). Such areas mainly represent urban sites, slope outcrops or rocky ranges, where the intensity of the scattered radiation is higher compared to rural areas wherein vegetated areas, meadows and crop fields suffer from temporal de-correlation of the radar signal. Furthermore, the applicability of this technique to landslide monitoring has further limitations, particularly the slope aspect which further limits applicability of the data for the analysis. This is also in addition to the previously mentioned lack of PS on vegetated and soil covered land.

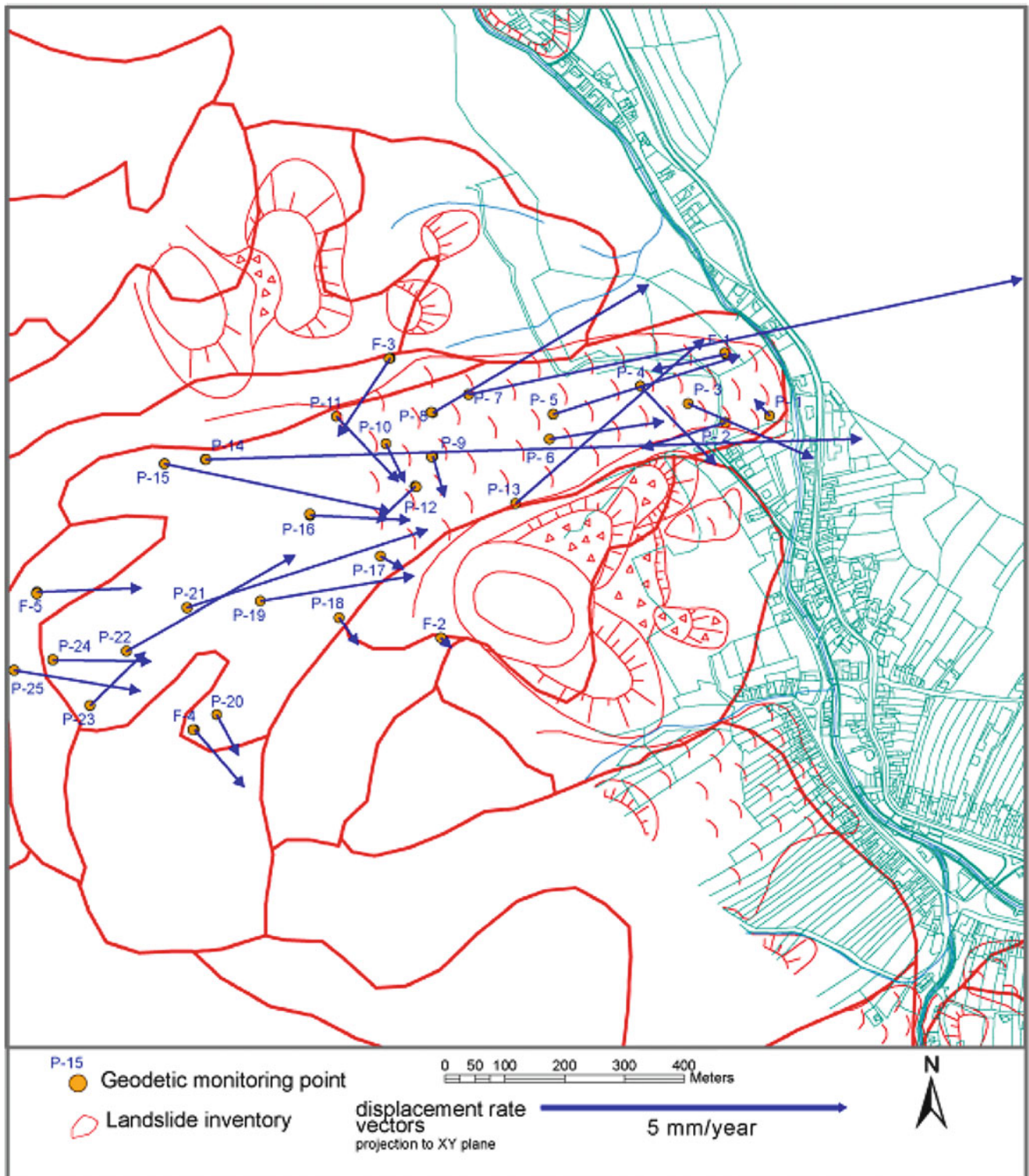


Fig. 2 Displacement rate vectors derived from the geodetic monitoring system of the catastrophic Lubietova landslide projected onto the horizontal plane showing differential deformation rates inside the landslide mass

The influence of atmospheric conditions on the accuracy of the PS results is well known, and to certain extent the

error can be removed using a statistical approach where there is availability of long-term data.

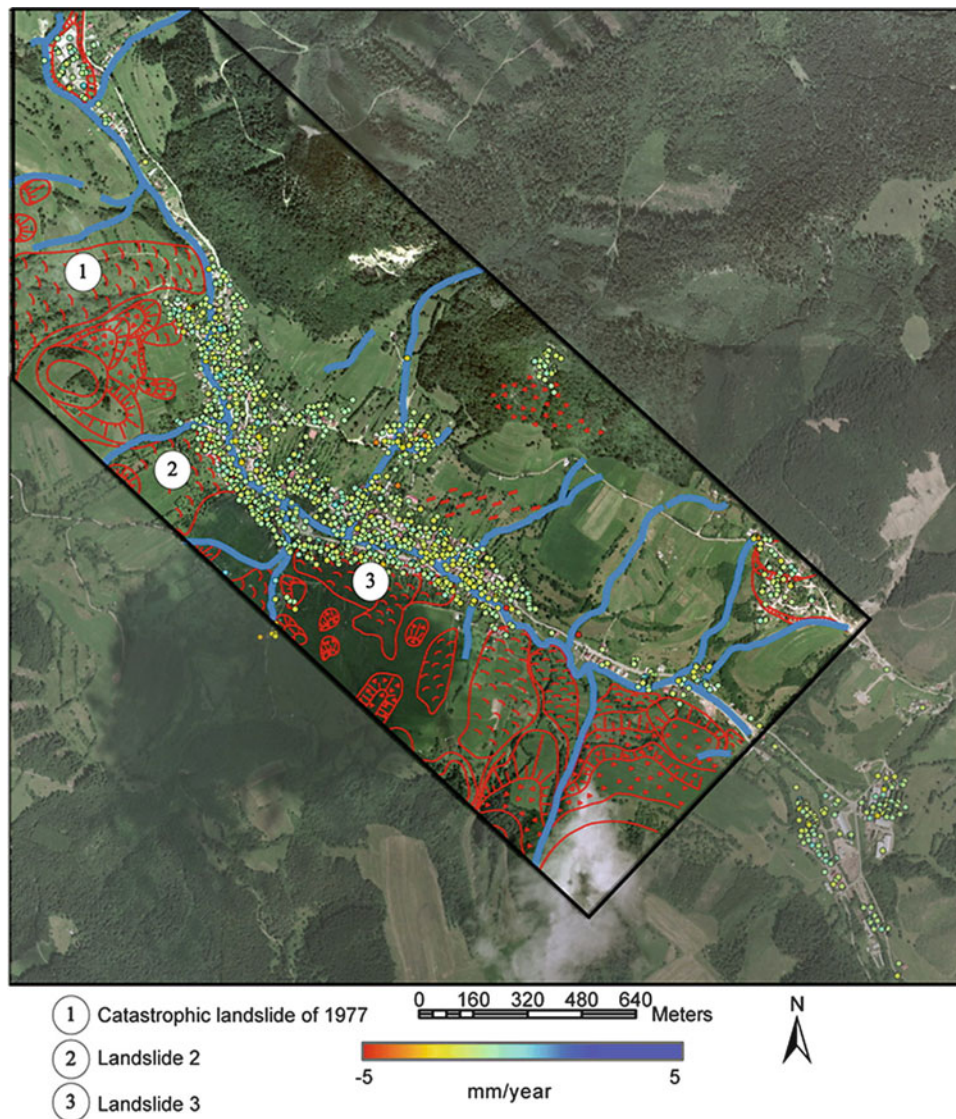


Fig. 3 Combined ERSd, ENVISAT, and LOS PS velocities in the Lubietova area showing the landslides in the vicinity of the town

The most important data for landslide monitoring are the displacement vectors derived from various sensors indicating the amplitude and direction of the deformations. The PS data represents the displacements in the line of sight direction of the radar sensor, and this is of limited use for the detection of the orientation in which the deformation progresses. In order to extract the horizontal component of the deformation along the line of the slope, a transformation of 1D LOS data has to take place, and this also further limits the applicable data mainly due to relative orientation of radar vision vector toward the slope orientation. The aspect angle and slope dip angle particularly affect the utility of the PS-InSAR data (Cascini et al. 2010).

Moduli of displacement rates in the slope direction were determined by the transformation of 1D LOS PS velocity rates in the accumulation zones of landslides L2 and L3. The

velocities for the active areas of the L2 landslide were less than 3 mm/year while in the L3 landslides it reached less than 20 mm/year. The later displacement rates must be approached with caution, since these were based only on ERS and ENVISAT descending orbits data with a scaling factor near 7. The data from the ascending ENVISAT acquisitions were discarded due to the high value of the scaling factor. Even though the PS-InSAR technique did not produce any usable targets within the L1 catastrophic landslide of 1977, the measured displacement rates for the L2 and L3 landslides in the immediate vicinity of the L1 landslide are comparable in magnitude to the results obtained by long-term geodetic monitoring recorded within the L1 landslide.

Furthermore, it was possible to redraw the boundaries of the L2 and L3 landslides based on the slope direction velocity

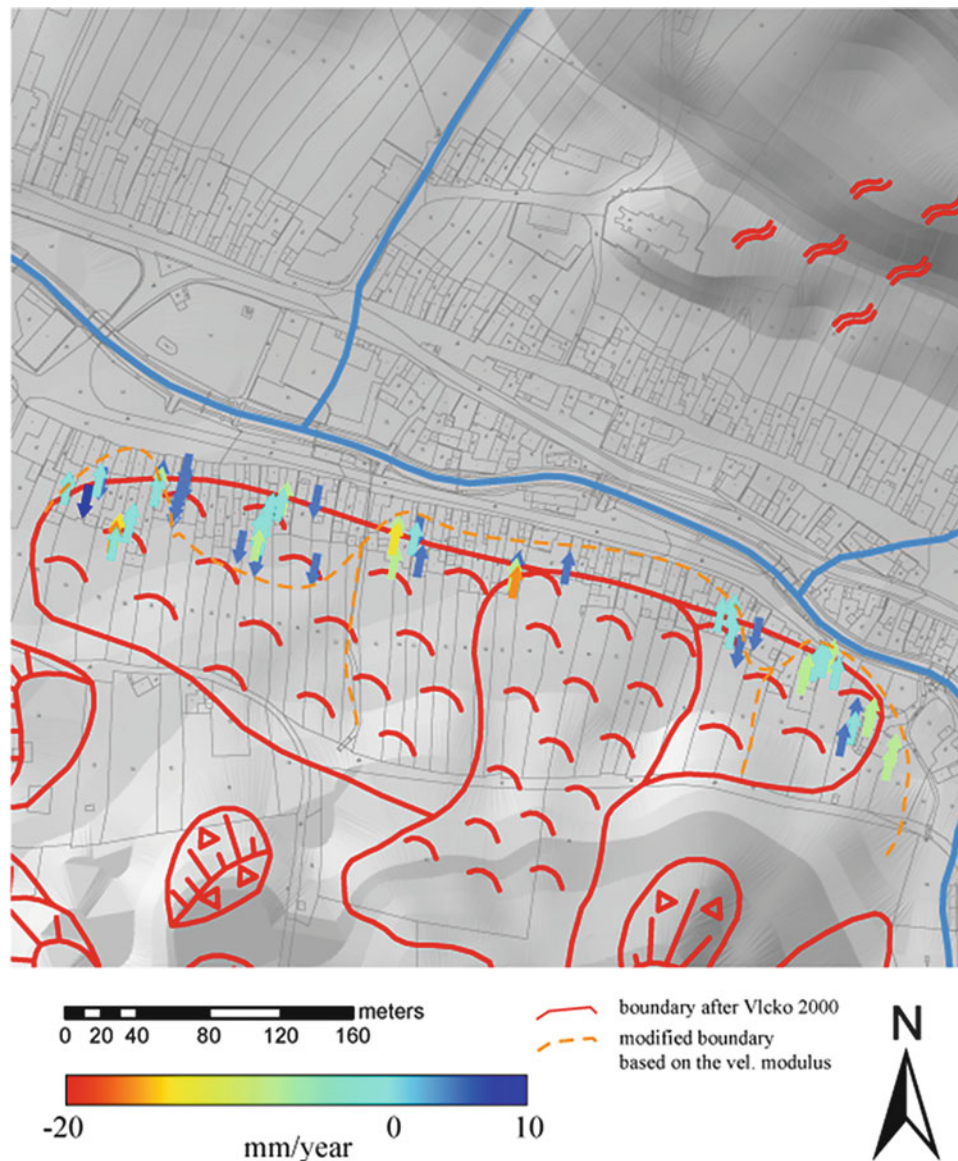


Fig. 4 Displacement rates transformed to the deepest slope orientation for the landslide L3 with the modified accumulation part of the landslide boundary according to the moduli of the displacement rates at the PS locations

moduli of displacements indicating different deformation rates within one sliding body (Fig. 4).

The PS-InSAR technique proved to be a valuable help in cases where it succeeds in producing sufficient densities of targets within the landslide mass.

An attempt to extract slope direction displacement rates from 1D LOS data was carried out, and this proved to have greater value in the landslide monitoring. However, it also indicated the limits for useful transformation of PS LOS displacement rates, with the slope aspect particularly heavily affecting successful application of this method. It would be beneficial to further automate the transformation procedure within the GIS in order to have the results to hand more

rapidly. This could be an area for future development of the PS technique in landslide monitoring practice.

All results obtained either with precise geodetic monitoring and with satellite interferometry indicate that the landslides located on the western bank of the Hutna River are in continuous slow creep movement, and they require constant monitoring even though the current threat to people and property is not considered to be very high.

Acknowledgments This work was supported by a grant from the Slovak Ministry of Education VEGA (contract no. 1/0331/09) and partly by the EU FP7 project “SAFER” (contract no. 218802) and Grant of the Slovak Research and Development Agency (contract no. DO7RP-0012-09, **APVV – 0330-10** and APVV-0641-10).

References

- Amelung F, Galloway DL, Bell JW, Zebker HA, Lacznik RJ (1999) Sensing the ups and downs of Las Vegas: InSAR reveals structural control of land subsidence and aquifer-system deformation. *Geology* 27(6):483–486
- Berardino P, Fornaro G, Lanari R, Sansosti E (2002) A new algorithm for surface deformation monitoring based on small baseline differential SAR interferograms. *IEEE Trans Geosci Remot Sens* 40(11):2375–2383
- Bovenga F, Nutricato R, Refice A, Wasowski J (2006) Application of multi-temporal differential interferometry to slope instability detection in urban/peri-urban areas. *Eng Geol* 88:219–240
- Cascini L, Fornaro G, Peduto D (2010) Advanced low- and full-resolution DInSAR map generation for slow-moving landslide analysis at different scales. *Eng Geol* 112(1–4):29–42
- Colesanti C, Wasowski J (2004) Satellite SAR interferometry for wide-area slope hazard detection and site-specific monitoring of slow landslides. In: *Proceedings ninth international symposium on landslides*, June 28–July 2 2004, Rio de Janeiro, pp 795–802
- Colesanti C, Wasowski J (2006) Investigating landslides with spaceborne synthetic aperture radar (SAR) interferometry. *Eng Geol* 88:173–199
- Colesanti C, Ferretti A, Prati C, Rocca F (2003) Monitoring landslides and tectonic motion with the Permanent Scatterers Technique. *Eng Geol* 68:1–14
- Crosetto M, Crippa B, Biescas E (2005) Early detection and in-depth analysis of deformation phenomena by radar interferometry. *Eng Geol* 79(1–2):81–91
- Farina P, Colombo D, Fumagalli A, Marks F, Moretti S (2006) Permanent scatterers for landslide investigations: outcomes from the ESA-SLAM project. *Eng Geol* 88:200–217
- Farina P, Casagli N, Ferretti A (2008) Radar-interpretation of InSAR measurements for landslide investigations in civil protection practices. In: *Proceedings of the 1st North American landslide conference*, Vail, 3–7 June 2007, pp 272–283
- Ferretti A, Prati C, Rocca F (1999) Multibaseline InSAR DEM reconstruction: the wavelet approach. *IEEE Trans Geosci Remot Sens* 37(2):705–715
- Ferretti A, Prati C, Rocca F (2000) Non-linear subsidence rate estimation using permanent scatterers in differential SAR interferometry. *IEEE Trans Geosci Remot Sens* 38(5):2202–2212
- Ferretti A, Prati C, Rocca F (2001) Permanent scatterers in SAR interferometry. *IEEE Trans Geosci Remot Sens* 39(1):8–20
- Fornaro G, Pauciuolo A, Serafino F (2007) Multipass SAR processing for urbanized areas imaging and deformation monitoring at small and large scales. In: *Proceedings of urban remote sensing joint event URS 2007 Paris*, 11–13 April
- Fruneau B, Achache J, Delacourt C (1996) Observation and modelling of the Saint-Etienne-de-Tienne landslide using SAR interferometry. *Tectonophysics* 265:181–190
- Gabriel AK, Goldstein RM, Zebker HA (1989) Mapping small elevation changes over large areas: differential radar interferometry. *J Geophys Res* 94(B7):9183–9191
- Guarnieri AM, Tebaldini S (2008) On the exploitation of target statistics for SAR interferometry applications. *IEEE Trans Geosci Remot Sens* 46(11):3436–3443
- Hasager CHB, Jensen NO, Nielsen M, Furevik B (2002) SAR satellite image derived wind speed maps validated with in-situ meteorological observations and footprint theory for offshore wind resource mapping. In: *2002 global windpower proceedings 2–5 April 2002, CNIT – La Défense – Paris – France*. Available also online: http://sitecoremedia.risoe.dk/research/vea/Documents/globalwindpower2002_proceedings.pdf. Accessed 4 May 2010
- Henry E, Mayer C, Rott H (2004) Mapping mining-induced subsidence from space in a hard rock mine: example of SAR interferometry application at Kiruna mine. *CIM Bull* 97(1083):1–5
- Herrera G, Davalillo JC, Cooksley G, Monserrat O, Pancioli V (2009) Mapping and monitoring geomorphological processes in mountainous areas using PSI data: Central pyrenees case study. *Nat Hazards Earth Syst* 9:1587–1598
- Hilley GE, Bürgmann R, Ferretti A, Novali F, Rocca F (2004) Dynamics of slow-moving landslides from permanent scatterer analysis. *Science* 304:1952–1955
- Jadroň D, Fussgänger E, Banský M, Tyleček B, Malgot J, Fekáč J, Frnčo M (1975) Lubietova landslide – detailed survey. Final report, 106 p (in Slovak)
- Kampes BM, Adam N (2005) The STUN algorithm for persistent scatterer interferometry. In: *Fringe 2005 Workshop, Frascati*. http://earth.esa.int/fringe2005/proceedings/papers/58_kampes.pdf. Accessed 19 Jan 2009
- Malet JP, Maquaire O, Calais E (2002) The use of global positioning system techniques for the continuous monitoring of landslides – application to the super – sauze earth flow (Alpes de Haute-Provence, France). *Geomorphology* 43:33–54
- Malgot J (1978) Slope deformations in the vicinity of Lubietova. *Geol Průzkum* 20(1):11–14 (in Slovak)
- Manzo M, Ricciardi GP, Casu F, Ventura G, Zeni G, Borgstrom S, Berardino P, Del Gaudio C, Lanari R (2006) Surface deformation analysis in the Ischia Island (Italy) based on spaceborne radar interferometry. *J Volcanol Geoth Res* 151(4):399–416
- Mika R (1999) Assessment of the Lubietova landslide stability. In: Klukanová A (ed) in Slovak. GSSR, Bratislava, pp 54–58, in Slovak
- Mora O, Mallorqui JJ, Broquetas A (2003) Linear and nonlinear terrain deformation maps from a reduced set of interferometric SAR images. *IEEE Trans Geosci Remot Sens* 41(10):2243–2253
- Nemčok A (1982) Landslides in slovak carpathians. Veda, vyd SAV, Bratislava, p 319, in Slovak
- Novali F, Ferretti A, Prati C, Rocca F, Savio G, Musazzi S (2005) PSInSAR validation by means of a blind experiment using dihedral reflectors. In: *Proceedings FRINGE 2005, Frascati*, 28 Nov–2 Dec 2005, ESASP-610. Available also online: http://earth.esa.int/workshops/fringe2005/proceedings/papers/253_novali.pdf. Accessed 9 Dec 2009
- Prokesova R, Kardos M, Medvedova A (2010) Landslide dynamics from high-resolution aerial photographs: a case study from the Western Carpathians, Slovakia. *Geomorphology* 115:90–101
- Righini G, Del Ventisette C, Constantini M, Malvarosa F, Minati F (2009) Spaceborne SAR analysis for landslides mapping in the framework of the PREVIEW project. In: Sassa K, Canuti P (eds) *Landslides: disaster risk reduction*. Springer, Berlin, pp 299–301
- Rocca F (2003) 3D motion recovery with multi-angle and/or left right Interferometry. In: *Proceedings 3rd international workshop on ERS SAR interferometry, FRINGE 2003, Frascati*, 2–5 Dec 2003. ESA SP-550. Available also online: http://earth.esa.int/fringe03/proceedings/posters/62_rocca.pdf. Accessed 6 Mar 2009
- Rott H, Nagler T (2006) The contribution of radar interferometry to the assessment of landslide hazards. *Adv Space Res* 37(4):710–719
- Rott H, Scheuchl B, Siegel A, Grasemann B (1999) Monitoring very slow slope movements by means of SAR interferometry: a case study from a mass waste above a reservoir in the Ötztal Alps, Austria. *Geophys Res Lett* 26:1629–1632
- Rott H, Nagler T, Rocca F, Prati C, Mazzotti A, Keusen HR, Liener, Tarchi D (2002) MUSCL – monitoring urban subsidence, cavities and landslides by remote sensing. Final Report, EC Project EVG1-CT-1999-00008, Institute for Meteorology and Geophysics, University of Innsbruck, Austria
- Rott H, Nagler T, Rocca F, Prati C, Mazzotti A, Keusen HR, Liener, Tarchi D (2003) InSAR techniques and applications for monitoring

- landslides and subsidence. In: Benes (ed) Geoinformation for European-wide integration, proceedings of EARSeL assembly, Prague, June 2002, Millpress, Rotterdam 25–31
- Singhroy V (2009) Satellite remote sensing applications for landslide detection and monitoring. In: Sassa K, Canuti P (eds) Landslides: disaster risk reduction. Springer, Berlin, pp 143–158
- Singhroy V, Mattar KE, Gray AL (1998) Landslide characteristics in Canada using interferometric SAR and combined SAR and TM images. *Adv Space Res* 3:465–476
- Van der Kooij M (1999) Engineering geology landslide investigations and SAR Interferometry. In: Proceedings of FRINGE'99, Liege
- Vietmeier J, Wagner W, Dikau R (1999) Monitoring moderate slope movements (landslides) in the southern French Alps using differential SAR interferometry. In: Proceedings of Fringe '99, Lieges
- Vlcko J, Maas P, Ayele T (2001) Assessment of the engineering geological conditions of Lubietova village for the urbanization purposes. Final report, p 20 (in Slovak)
- Wegmüller U, Werner C, Strozzi T, Wiesmann A (2005) ERS – ASAR integration in the interferometric point target analysis. In: Proceedings Fringe 2005 workshop, Frascati, 28 Nov–2 Dec. http://earth.esa.int/workshops/fringe05/proceedings/papers/196_wegmuller.pdf. Accessed 6 Mar 2009
- Ye X, Kaufmann H, Guo XF (2004) Landslide monitoring in the three gorges area using D-InSAR and corner reflectors. *Photogramm Eng Rem S* 70(10):1167–1172

Landslide Science and Practice

Volume 2: Early Warning, Instrumentation and
Monitoring

Margottini, C.; Canuti, P.; Sassa, K. (Eds.)

2013, XIX, 685 p. 755 illus., 669 illus. in color.,

Hardcover

ISBN: 978-3-642-31444-5